2016 23rd International Conference on Pattern Recognition (ICPR)
Cancún Center, Cancún, México, December 4-8, 2016

Fast Motion Deblurring using Gyroscopes and Strong Edge Prediction

Jiacai Zhao, Jie Ma*, Bin Fang, Siwen Quan and Fangyu Hu
Guangdong HUST Industrial Technology Research Institute, Guangdong Province Key Lab of Digital Manufacturing Equipment
National Key Laboratory of Science and Technology on Multi-spectral Information Processing
School of Automation, Huazhong University of Science and Technology
Wuhan, Hubei 430074, China
{zhaojc_hust, lisben_cyan, hufangyu_hust}@163.com, {majie, siwenquan}@hust.edu.cn

***Abstract*—This paper presents a fast deblurring algorithm to remove camera motion blur from a single photograph using built-in gyroscopes and strong edge prediction. An inaccurate blur kernel or point spread function (PSF) usually leads to an unsatisfying restored result. Hence, we propose a robust three-phase method for accurate PSF estimation. In the first stage, we utilize the embedded gyroscopes to compute a coarse version of the PSF from the camera's angular velocity during an exposure. In order to reduce the execution time of the later PSF modification, we introduce a patch selection procedure in the second stage to choose a suitable region from the blurry image based on the size of the coarse PSF estimated in stage one. The third phase aims to modify the coarse PSF to obtain an accurate one by predicting strong edges from an estimated latent image. In our experiments, we compare the restoration performance of several state-of-the-art approaches including ours and find that the proposed method outperforms others qualitatively as well as quantitatively. In addition, our method is also compared with the multi-scale approach without gyroscope data and shows shorter processing time and comparable deblurring quality. To the best of our knowledge, this is the first work that combines the sensor-aided method with the image-based approach to estimate the blur kernel.**

Keywords—motion blur; deblurring; gyroscopes; strong edge prediction; point spread function (PSF)

I. INTRODUCTION

A motion blur, caused by relative motion between the camera and the image scene during an exposure, is one of the most frequent problems in photography especially under a poor illumination condition. The goal of motion deblurring is just to restore the latent sharp image of the scene from the captured blurry image. Motion deblurring is recognized as a complex and challenging problem and has been hotly discussed for a long time in the computer vision and graphics community. Until recently, a lot of image restoration methods have been proposed and perform well in motion deblurring.

Most existing motion deblurring algorithms assume that the image blur is spatially invariant. Under this assumption, a blurry image B can be modeled as the convolution of a latent sharp image I with a shift-invariant point spread function (PSF) or blur kernel K:

$$B = I \otimes K + N, \tag{1}$$

where N is the noise and $\otimes$ denotes the convolution operator. To reconstruct the latent sharp image, we first need accurate knowledge of the blur kernel. In recent years, a lot of effective approaches have been proposed for kernel estimation. In general, we can divide these methods into two main categories: sensor-aided methods and image-based approaches.

Sensor-aided methods utilize the embedded inertial sensors to directly measure the camera motion for PSF estimation. Joshi et al. [1] used an inertial measurement unit to measure the camera's angular velocity and acceleration and computed the blur kernel by reconstructing the camera's motion path, which was followed by related research in [2-5]. These methods can easily handle large image blurs and run fast even on high-resolution images. However, significant error, known as 'drift' and noise, exists when tracking the camera motion using the inertial sensors, which finally results in inaccurate motion path and undesirable blur kernel. Beyond that, it is not an easy task to achieve accurate camera calibration and synchronization between the camera and gyroscope samples.

Image-based methods estimate the blur kernel directly from the blurry image using a parametric model. Fergus et al. [6] utilized a variational Bayesian framework based on heavy-tailed natural image prior to estimate the blur kernel. Shan et al. [7] also used a probabilistic model of both the blur kernel and latent sharp image. Joshi et al. [8] predicted sharp edges of a blurry image for PSF estimation and similar approaches are applied in [9-11]. Krishnan et al. [12] proposed to use the ratio of the L_1 norm to the L_2 norm on the high frequencies of an image as the regularization function for blind kernel estimation. Although these methods can provide satisfying restored results, they usually have long run times since a multi-scale scheme is usually used for kernel estimation.

As described above, both the sensor-aided and image-based methods have their own limitations. However, little attention has been devoted to combine them. In this paper, we propose a robust and efficient method taking the advantages of above two methods to estimate the blur kernel. First, we use the embedded gyroscopes to measure the camera's angular velocity during the

*Jie Ma is the corresponding author. This work was supported in part by the Guangdong Innovative and Entrepreneurial Research Team Program under Grant 2014ZT05G304, Astronautical Supporting Technology Foundation of China CASC2014 and CALT2014, Innovation Research Fund of Huazhong University of Science and Technology.

exposure period and compute an initial PSF by reconstructing the camera's motion path. Then, we select a suitable image patch from the blurry image for PSF modification. Last, we modify the initial PSF with the selected patch to obtain its accurate version based on strong edge prediction. The proposed algorithm is completely automatic, robust and fast, and can run on any photographic device with gyroscopes, e.g. smartphones, digital cameras. The main contributions of the proposed research are listed as follows:

1) We integrate the sensor-aided method with the image-based approach to obtain an accurate PSF within a short time. The proposed method can be applied to any photographic device with gyroscopes.

2) We propose a novel adaptive patch selection method to choose a sub-region from the blurry image for PSF estimation taking consideration of the processing time.

We applied the proposed method to real photos from a smartphone with gyroscopes and analyzed the restoration performance of several deblurring algorithms including ours. Experimental results demonstrated that our method performed better than other existing methods.

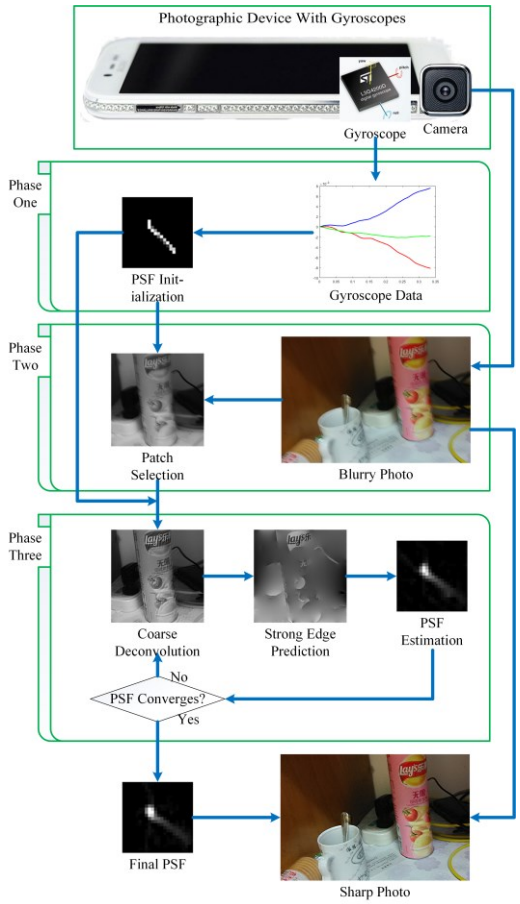

Fig. 1. Proposed framework for motion debluring. *(For visualization, the image in "Strong Edge Prediction" has been restored from the predicted gradient maps by Poisson reconstruction.)*

The remainder of this paper is organized as follows: Section 2 discusses the proposed algorithm. Section 3 shows the experimental results including the qualitative and quantitative comparison with the state-of-the-art deblurring methods. The multi-scale approach without gyroscope data is also examined. Section 4 presents the conclusion.

II. ALGORITHM

The proposed deblurring algorithm to remove camera motion blur is depicted in Fig. 1. First, A photograhic device with gyroscopes (e.g., a smartphone) is used to capture a blurry photo and the gyroscope data. Then, two main steps, including PSF estimation and image deconvolution, are taken to deblur the captured blurry photo. In the first step of PSF estimation, we introduce a three-phase method to estimate an accurate PSF, including (1) PSF initialization, (2) patch selection and (3) PSF modification. In the second step of image deconvolution, we use a simple but fast Wiener filter to recover the latent sharp image in consideration of the processing time. More details of the proposed algorithm will be discussed in this section.

A. Three-Phase PSF Estimation

Existing image-based PSF estimation methods usually perform well in image quality but badly in the execution time while the sensor-aided methods have short execution time but low accuracy. Taking the advantages of above two methods, we propose a three-phase method to estimate the blur kernel. In the first stage, we efficiently compute a coarse PSF by reconstructing the motion path using the gyroscope data. In the second stage, we select a sub-region from the blurry image to reduce the processing time of the later PSF modification. In the third stage, we modify the coarse PSF to obtain its accurate version using strong edge prediction.

1) *Phase One: PSF Initialization:* In this paper, the camera motion is only modeled as a rotation. We ignore translations because camera motion blur primarily results from rotations. Moreover, we must integrate accelerometer data twice to obtain translations, during which process significant error usually occurs. Thus, we take no consideration of translations in our model.

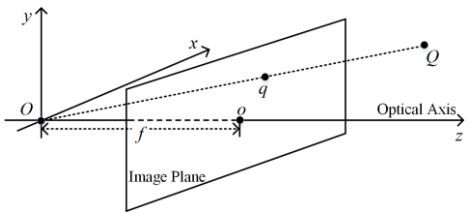

Fig. 2. Pinhole camera model. *(A ray from the camera center O to an object point Q in the image scene will intersect the image plane at point q.)*

Our rotational camera model is based on the pinhole camera model, as shown in Fig. 2. If the camera shakes during the exposure peroid, the projection point q in the image plane, corresponded with the object point Q in the image scene, will move with the camera and generate the motion path. The blur kernel is only related to the relative poisition of the camera during an exposure. If the embedded gyroscope samples K different rotations in this period, K different projection points

$q_k(x_k, y_k), k = 0,1,2,...,K-1$ will be computed as:

$$(x_k, y_k)^T = \prod\left(CR_k C^{-1}(x_0, y_0, 1)^T\right). \quad (2)$$

Here C is the camera intrinsic matrix and R_k is the rotation matrix. $\prod(\cdot)$ denotes a projection that transforms a point (x, y, z) in the 3-D space to the corresponding point (x', y') in the image plane:

$$\prod\left((x, y, z)^T\right) = (x/z, y/z)^T. \quad (3)$$

For simplicity, we assume that the optical axis of the camera is aligned with the z axis and the camera intrinsic matrix C is only related to the focal length f of the camera. The image blur is assumed to be spatially invariant. Then we get the simplification of (2):

$$(x_k, y_k)^T = (x_0, y_0)^T + f \cdot (\theta_k^y, \theta_k^x)^T, \quad (4)$$

where θ_k^x and θ_k^y represent the k th camera orientation around x and y axis, which can be obtained by integrating gyroscope data only once. To improve the kernel's accuracy, we can interpolate the camera orientation from known samples.

2) *Phase Two: Patch Selection:* The coarse PSF estimated in phase one is usually inaccurate due to its involvements of many challenges in accurate motion measurement, camera calibration and synchronization between the camera and gyroscope data. Therefore, we propose a PSF modification procedure to correct the coarse PSF to obtain its version using an image-based method. It takes a long time to process the entire image for the kernel modification. Yang et al. [13] proposed to use the Harris corner detector to choose a small patch from the blurry image to estimate the blur kernel. But corners are not always beneficial for kernel estimation. In this section, we propose a novel adaptive patch selection method by measuring the usefulness of image edges in motion deblurring.

In [10], Xu et al. found that not all strong edges are useful for PSF estimation. Only the large-scale object that's wider than the kernel can yield stable kernel estimation. They proposed a new metric to measure the usefulness of image edges in motion deblurring, which was define as

$$r(x) = \frac{\left\|\sum_{y \in N_h(x)} \nabla B(y)\right\|}{\sum_{y \in N_h(x)} \left\|\nabla B(y)\right\| + 0.5}, \quad (5)$$

where $N_h(x)$ is a $h \times h$ window centered at pixel x, and the constant 0.5 is to prevent producing a larger r in flat regions.

A small r implies either a flat region or small-scale object, which is exactly not suitable for kernel estimation. To measure the fitness of a region being the patch, we introduce a fitness function defined as

$$f(p) = \frac{1}{Z_p} \sum_{x \in W_p} r(x), \quad (6)$$

where W_p is a $w \times w$ window centered at pixel p, Z_p is a normalization term. A higher fitness value at pixel p means that the region around p contains more large-scale objects profiting the kernel estimation.

In order to filter out smaller-scale objects in the input blurry image, the size of the window $N_h(x)$ is set to the coarse PSF estimated in phase one. The size of the window W_p is set to the patch size, which is also related to the blur kernel. Considering both the processing time and stability of kernel estimation, we set the edge length of the patch to 20 of the coarse PSF.

As shown in Fig. 3, we compare the deblurring results of five different patch selection approaches, including (1) our method, (2) Yang's method [13], (3) the region with maximum gradient magnitude, (4) the central region and (5) the whole image. As shown in Fig. 3(b), using our method finds the patch with many large-scale objects and produces a satisfying deblurring result. Using (2) and (3) usually finds the similar region containing many spikes or narrow objects and yields unstable kernel estimation, as shown in Fig. 3(c)-(d). Using the central region usually finds the most salient part of an image and needs no additional computation. However, sometimes the central region may be flat or contain many narrow objects and makes the kernel estimation ambiguous. Using the whole image usually produces the best restored result but has a long execution time, as shown in Fig. 3(f). With the proposed method, we can find a suitable region containing as many large-scale objects as possible to profit the kernel estimation.

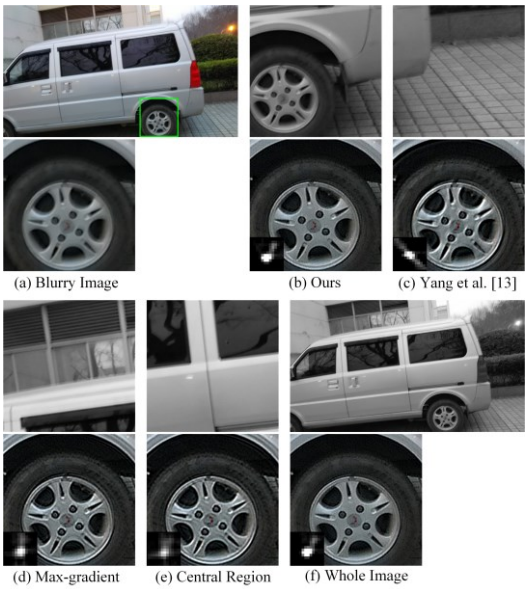

Fig. 3. Different patch selection methods and the corresponding deblurring result. *((a) the blurry image and its local window. (b)-(f) the selected patches of different methods and deblurring results of the local window.)*

3) *Phase Three: PSF Modification using Strong Edge Prediction:* In this section, we introduce a method to modify the coarse PSF to obtain an accurate one with the patch B_p selected in phase two. What's different from existing image-based method is that we need neither define the initial kernel

size or use a multi-scale scheme since the initial PSF has been estimated in the first stage. The proposed PSF modification method directly corrects the coarse blur kernel with an iterative process on the selected patch. Each iteration can be divided into three main steps – that is, coarse image deconvolution, strong edge prediction and PSF estimation.

a) Coarse Image Deconvolution: Given a blur kernel K, we solve for a coarse version of the latent image patch I_p from the selected blurry image patch B_p by minimizing the energy function:

$$E(I_p) = \|I_p \otimes K - B_p\|^2 + \lambda \|\nabla I_p\|^2 . \quad (7)$$

A conjugate gradient (CG) method can be taken to solve the problem. The closed-form solution exists and is given as

$$I_p = F^{-1}\left(\frac{\overline{F(K)} F(B_p)}{\overline{F(K)} F(K) + \lambda \left(\overline{F(\partial_x)} F(\partial_x) + \overline{F(\partial_y)} F(\partial_y) \right)} \right), \quad (8)$$

where $F(\cdot)$ and $F^{-1}(\cdot)$ denote the FFT and inverse FFT respectively. $\overline{F(\cdot)}$ is the complex conjugate operator. λ is the regularization weight controlling the smoothness of I_p.

b) Strong Edge Prediction: In the prediction step, we estimate the strong edges I_p^s of the latent image patch I_p. First we perform bilateral filtering [14] to the current latent image patch I_p to suppress the noise. Then A shock filter [15] is used to reconstruct the strong edges of I_p. The shock filtered image contains not only sharp edges but also enhanced noise. So a threshold filter is performed to suppress the enhanced noise, whose evolution equation is formulated as

$$\nabla I_p^s = \nabla I_p \cdot H\left(\|\nabla I_p\| - \tau \cdot M\left(\|\nabla I_p\| \right) \right), \quad (9)$$

where $H(\cdot)$ and $M(\cdot)$ denote the Heaviside step function and the maximum function respectively. τ is a threshold.

c) PSF Estimation: To estimate the blur kernel K using the predicted strong edges I_p^s, we minimize the energy function:

$$E(K) = \|\nabla I_p^s \otimes K - \nabla B_p\|^2 + \gamma \|K\|^2 , \quad (10)$$

where γ is the adjustable weight to control the sparseness of the blur kernel. The close-form solution for K is given by

$$K = F^{-1}\left(\frac{\overline{F(\partial_x I_p^s)} F(\partial_x B_p) + \overline{F(\partial_y I_p^s)} F(\partial_y B_p)}{\overline{F(\partial_x I_p^s)} F(\partial_x I_p^s) + \overline{F(\partial_y I_p^s)} F(\partial_y I_p^s) + \gamma} \right). \quad (11)$$

At the end of each of each iteration, we set elements with values smaller than 1/50 of the biggest one to zeros and preserve the maximum component for kernel denoising. Then, we normalize K to make the sum of the blur kernel to be one.

It's important that iterative PSF modification converges in a limited number of iterations. Fig. 4 shows the convergence speed of the iterative process. The graph shows that the change rate of PSF drastically decreases to near zero only in a few iterations, where the change rate of PSF is measured by the sum of pixel-wised squared differences between the estimated kernels of two adjacent iterations. It means that the estimated kernel has little change after several iterations and the iterative PSF modification converges fast. The visualized kernels also show that the estimated kernel has no significant change after a few iterations are performed.

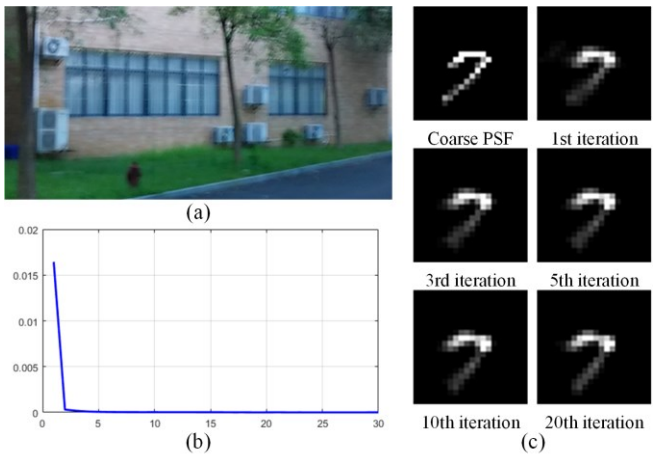

Fig. 4. Convergence speed of iterative PSF modification. *((a) blurry image. (b) the change rate of PSF (vertical) vs. number of iterations in PSF modification. (c) estimated kernels after different numbers of iterations.)*

B. Final Image Deconvolution

We can recover the latent sharp image from the blurry input image with the accurate estimated PSF. Most state-of-the-art non-blind deconvolution algorithms require computationally expensive iterative optimization. To remove the camera motion blur in a short time, we use a simple Wiener filter in the form

$$\hat{I} = F^{-1}\left(\frac{1}{F(K)} \frac{|F(K)|^2}{|F(K)|^2 + \eta} F(B) \right), \quad (12)$$

where $\hat{I}$ is the estimated latent image and η is an estimation of the signal-to-noise ratio.

III. Experimental Result

In our experiments, we first use a smartphone with Android OS to capture various kinds of real photos. Then we utilize a personal computer with MATLAB R2016a to estimate the blur kernel and reconstruct the latent sharp image. The experimental computer is equipped with 3.30GHz CPU and 8GB RAM. Fig. 5 shows our main experimental workflow. In PSF modification step, the parameter λ in (7) is set to 0.01, τ in (9) is set to 0.2 and γ in (10) is set to 80. In final image deconvolution step, the parameter η in (12) is set to 0.01. Considering the execution time and the accuracy of PSF, we perform seven iterations when modifying the coarse PSF.

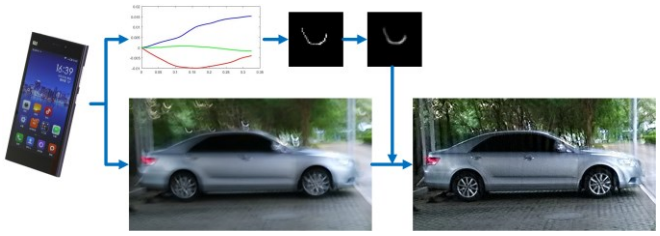

Fig. 5. Basic experimental workflow

Our method is compared with two types of state-of-the-art methods including sensor-aided method [3] and image-based approaches [7,9,12] , qualitatively as well as quantitatively. Fig. 6 shows the restoration results of different image deblurring methods. Fig. 6(b) contains serious ringing artifacts when only gyroscope data is used. Fig. 6(c) and (e) contain large artifacts too. Although Fig. 6(d) removes more motion blur, it has unnatural discontinuities and intensity saturation. The result with our method outperforms others.

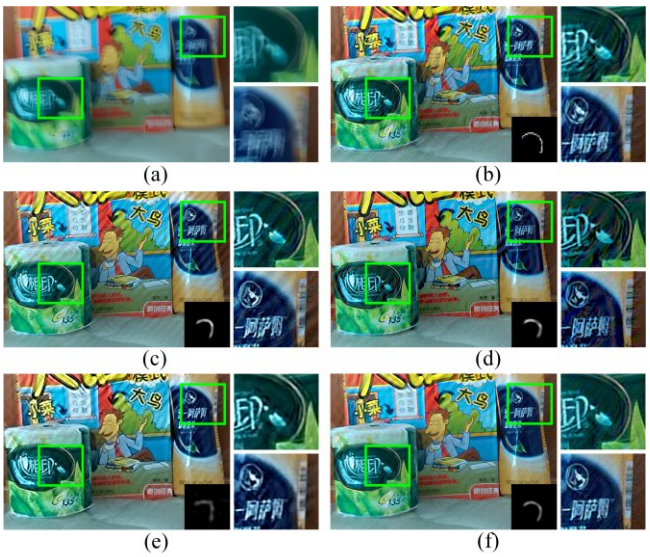

Fig. 6. Qualitative comparison of different image deblurring methods. *((a) blurry image. (b)-(e) deblurring results of [3],[7],[9] and [12]. (f) deblurring result of our method.)*

For quantitative comparison, we utilize the non-reference quality assessment method proposed in [16] to evaluate the quality of motion deblurring. A higher assessment score value implies higher deblurring quality. As shown in Fig. 7, we restore four 1280×720 real photos using different methods and compare the assessment scores. The graph shows that our method gets comparable or higher scores and performs the best.

Table I compares the processing times using five different deblurring methods for the deblurring examples in Fig. 7. Our method runs faster than others except Šindelář's method [3], in which only gyroscope data is used. For accuracy consideration, our method performs an additional iterative process to correct the coarse kernel.

Our method is also compared with the approach without gyroscope data. When using no gyroscope data, we utilize a multi-scale scheme to estimate the blur kernel in a coarse-to-fine process. At each scale, we perform the same iterative process with the proposed method to update the blur kernel and latent sharp image. For efficiency comparison, we use the whole image to estimate the blur kernel without patch selection procedure and apply the Wiener filter to recover the latent sharp image for both methods. A limitation of multi-scale method is that we must define the initial kernel size while our method can estimate the coarse kernel using gyroscope data. Here, we set the initial kernel size to the coarse kernel. The difference of above two methods is that our method corrects the coarse kernel on original blurry image while the multi-scale approach updates the blur kernel on created image pyramid.

Table II compares the assessment scores and processing times of our method and the multi-scale approach without gyroscope data for the deblurring examples in Fig. 7. Our method shows comparable deblurring quality and shorter processing time. It's demonstrated that the gyroscope data is useful for estimating the coarse kernel and improving the computational efficiency.

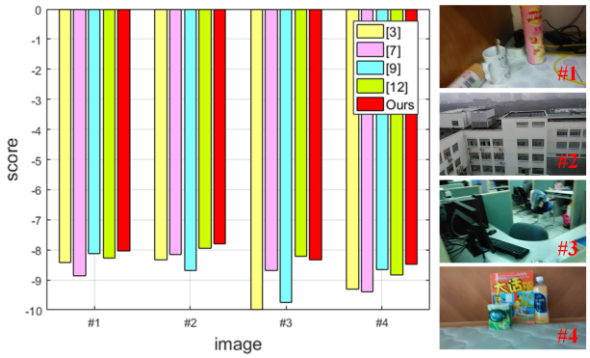

Fig. 7. Quantitative comparison of different image deblurring methods. *(Left: assessment scores of motion deblurring. Right: four real photos.)*

TABLE I. COMPARESION OF PROCESSING TIMES OF FIVE DIFFERENT METHODS (SEC.)

Real Photo	Method				
	[3]	*[7]*	*[9]*	*[12]*	*Ours*
#1	0.91	180.00	9.73	105.18	2.25
#2	0.81	182.00	9.79	104.26	1.72
#3	0.91	180.00	9.72	120.45	2.58
#4	0.94	181.00	9.84	93.95	3.21

TABLE II. COMPARESION OF RESTORATION PERFORMANCE OF TWO DIFFERENT METHODS

Real Photo	Kernel Size	Score		Processing Time (Sec.)	
		Multi-scale	*Ours*	*Multi-scale*	*Ours*
#1	25×25	-8.53	-8.49	9.00	5.25
#2	21×21	-8.16	-8.04	10.40	4.91
#3	29×29	-8.80	-8.51	11.35	5.26
#4	33×33	-8.69	-8.73	10.01	5.33

IV. CONCLUSION

In this paper, we have proposed a novel motion deblurring method to remove camera motion blur from a single blurry image. It's completely automatic, robust and fast, and can be applied to any photographic device with gyroscopes. This is the first work that attempts to integrate the sensor-aided method with the image-based approach to estimate the blur kernel. The combination of the two methods has several advantages compared with either of them, which are listed as follows:

1) It successfully combines the computational efficiency of the sensor-aided method with the accuracy of the image-based approach.

2) It overcomes several problems of the sensor-aided method, such as inaccurate camera calibration, difficult synchronization between camera and gyroscope data and significant measurement error.

3) It breaks through several limitations of the image-based method, such as additional user parameter and the multi-scale scheme.

In order to further reduce the execution time, we propose a novel adaptive patch selection method to choose a sub-region from the blurry image for the kernel modification. The experimental results demonstrate that our method performs better than the state-of-the-art image deblurring methods qualitatively as well as quantitatively. In addition, the gyroscope data profits coarse kernel estimation and computational efficiency. In the future work, we would like to take the camera translation into consideration for further improving the accuracy of the coarse kernel.

REFERENCES

[1] N. Joshi, S. B. Kang, C. L. Zitnick and R. Szeliski, "Image deblurring using inertial measurement sensors," *ACM Transactions on Graphics*. vol.29, no. 4, 2010.

[2] S. Park and M. Levoy, "Gyro-based multi-image deconvolution for removing handshake blur," in *Proceedings of the IEEE Conference on Computer Vision and Pattern Recognition*, 2014.

[3] O. Šindelář and F. Šroubek, "Image deblurring in smartphone devices using built-in inertial measurement sensors," *Journal of Electronic Imaging*, vol. 22, no. 1, 2013.

[4] E. Lee, E. Chae, H. Cheong and J. Paik, "Fast Motion Deblurring Using Sensor-Aided Motion Trajectory Estimation," *The Scientific World Journal*, 2014.

[5] R. Zhen and R. L. Stevenson, "Multi-image motion deblurring aided by inertial sensors," *Journal of Electronic Imaging*, vol. 25, no. 1, 2016.

[6] R. Fergus, B. Singh, A. Hertzmann, S. Roweis, and W. Freeman, "Removing camera shake from a single photograph," *ACM Transactions on Graphics*, vol. 25, no. 3, pp. 787-794, 2006.

[7] Q. Shan, J. Jia and A. Agarwala, "High-quality motion deblurring from a single image," *ACM Transactions on Graphics*, vol. 27, no. 3, 2008.

[8] N. Joshi, R. Szeliski and D. Kriegman, "PSF estimation using sharp edge prediction," in *Proceedings of the IEEE Conference on Computer Vision and Pattern Recognition*, 2008.

[9] S. Cho and S. Lee, "Fast motion deblurring," *ACM Transactions on Graphics*, vol. 28, no. 5, pp. 145-145, 2009.

[10] L. Xu and J. Jia, "Two-phase kernel estimation for robust motion deblurring," in *Proceedings of the 11th European Conference on Computer Vision*, 2010.

[11] X. Zhang, R. Wang, Y. Tian, W. Wang and W. Gao, "Image deblurring using robust sparsity priors," in *Proceedings of the IEEE International Conference on Image Processing*, pp. 138-142, 2015.

[12] D. Krishnan, T. Tay, R. Fergus, "Blind deconvolution using a normalized sparsity measure," in *Proceedings of the IEEE Conference on Computer Vision and Pattern Recognition*, 2011.

[13] H. L. Yang, Y. H. Chiao, P. H. Huang and S. H. Lai, "Blind image deblurring with modified richardson-lucy deconvolution for ringing artifact suppression," *Advances in Image and Video Technology*, pp. 240-251, 2011.

[14] C. Tomasi, R. Manduchi, "Bilateral filtering for gray and color images," in *Proceedings of the IEEE International Conference on Computer Vision*, pp. 839-846, 1998.

[15] S. Osher and L. I. Rudin, "Feature-oriented image enhancement using shock filters," *SIAM Journal on Numerical Analysis*, vol. 27, no. 4, pp. 919-940, 1990.

[16] Y. Liu, J. Wang, S. Cho, A. Finkelstein and S. Rusinkiewicz, "A no-reference metric for evaluating the quality of motion deblurring" *ACM Transactions on Graph*ics, vol. 32, no. 6, 2013.